Title	On solving singular interface problems using the enriched partition-of-unity finite element methods
Author(s)	Lee, Chi King; Liu, X.; Fan, Sau Cheong
Citation	Lee, C. K., Liu, X., & Fan, S. C. (2003). On solving singular interface problems using the enriched partition-of-unity finite element methods. Engineering Computations, 20(8), 998-1022.
Date	2003
URL	http://hdl.handle.net/10220/19229
Rights	© 2003 Emerald Group Publishing Limited. This is the author created version of a work that has been peer reviewed and accepted for publication by Engineering Computations, Emerald Group Publishing Limited. It incorporates referee's comments but changes resulting from the publishing process, such as copyediting, structural formatting, may not be reflected in this document. The published version is available at: [Article DOI: http://dx.doi.org/10.1108/02644400310502991].

On solving singular interface problems using the enriched partition-of-unity finite element methods

[1]C. K. Lee*, X. Liu, and S. C. Fan

School of Civil and Environmental Engineering
Nanyang Technological University
Nanyang Avenue
Singapore 639798

*Emails: [1]ccklee@ntu.edu.sg

Pre-printed version of the paper appeared in the journal:
Engineering Computations, Vol. 20, No. 8, pp998-1022

Summary

It has been well recognized that interface problems often contain strong singularities which make conventional numerical approaches such as uniform *h*- or *p*-version of finite element methods inefficient. In this paper, the partition-of-unity finite element method (PUFEM) is applied to obtain solution for interface problems with severe singularities. In the present approach, asymptotical expansions of the analytical solutions near the interface singularities are employed to enhance the accuracy of the solution. Three different enrichment schemes for interface problems are presented, and their performances are studied. Compared to other numerical approaches such as *h*-*p* version of finite element method, the main advantages of the present method include (i) easy and simple formulation, (ii) highly flexible enrichment configurations, (iii) no special treatment needed for numerical integration and boundary conditions and (iv) highly effective in terms of computational efficiency. Numerical examples are included to illustrate the robustness and performance of the three schemes in conjunction with uniform *h*- or *p*-refinements. It shows that the present PUFEM formulations can significantly improve the accuracy of solution. Very often, improved convergence rate is obtained through enrichment in conjunction with *p*-refinement.

KEYWORDS: partition-of-unity finite element methods, enriched cover functions, asymptotic solution, interface singular problems

*Correspondence author

1. Introduction

For elliptic problems, it has been well recognised that singularities of the solution can be caused by changes in values of coefficients of the elliptic operators within the problem domain [1-3]. Typical example of this type of singularity is the interface problems in structural mechanics, in which the problem domains are made up of more than one material region. Due to the presence of singularities along the interface of different materials, the interface problems are notoriously difficult to solve. The conventional uniform *h*- or *p*-version of finite element methods (FEM) may fail to provide any practical engineering solution at a reasonable cost. Towards this end, many researchers presented different approaches to obtain solution more effectively. The most popular approach is the adaptive *h*-version of FEM [4-6], in which refined elements are employed near the singular points to subdue the sturdy effects. Albeit this approach requires no special formulation to treat the singularity, a nearly optimal mesh is critical to obtain an accurate solution in an efficient manner [7, 8]. To achieve that, it demands a reliable *a posteriori* error estimator and a good automatic mesh generation scheme. These two are the prerequisites. However, the presence of different material in separate sub-regions will inevitably complicate the process during the *a posteriori* error estimation and the optimal mesh generation. It renders the adaptive *h*-version of FEM unattractive. An alternative is to use *h-p* version of FEM [9]. In it, the size of elements and the order of approximation functions need to be increased simultaneously in a well designed manner. Very often, an optimal *h-p* refinement scheme is able to yield the highest possible convergence rate [9]. Nevertheless, the *h-p* approach demands some kinds of specially designed *geometric meshes* near the singular points. It is achievable without excessive effort only for problems having simple interface domain geometries. But it may become an impossible mission when facing a real complex problem.

The *partition-of-unity finite element method* (PUFEM) is a recently developed numerical method [10-13], which combines the merits of both the partition-of-unity concept and the well developed FEM. The PUFEM and its extended forms including the *generalized finite element method* [14-16] and the *extended finite element method* [17-19] are in fact generalized forms of the traditional FEM with particular emphasis on local enriching within a FEM setting. Its approximating solution consists of two parts: the *partition-of-unity (PU) functions* and the *cover functions*. In the present approach, the PU functions adopt the standard FE interpolation functions. It enables the essential boundary conditions to be imposed without any difficulties. On the other hand, the

cover functions are enriched through embracing some kinds of analytical functions to form an enhanced basis functions. As a result, the present PUFEM formulation has the advantages over other numerical methods as follows.

(1) Simple formulation

Reportedly, many meshless formulations encountered great difficulties in defining the essential boundary conditions [20-22]. Since the standard FE interpolation functions are adopted in the present formulation as the PU functions, the treatment for essential boundary conditions becomes a trivial task. Besides, implementation of the PUFEM procedures demands almost the same, if not less, effort as in the conventional FE procedures.

(2) Flexible enrichment/refinement schemes

Similar to the *p*-type refinement strategy, improved solution is achieved by adopting a better approximation function. In the PUFEM, the accuracy of solution can be improved simply by adding more terms to enhance the basis of the nodal cover function. As such, the enrichment process can be carried out easily in a node-by-node manner. In the case of interface problems, the enrichment can be implemented in many ways, such as *single enrichment scheme*, *multi enrichment scheme* and *interface enrichment scheme*. More details of these enrichment schemes and their performance are elaborated in Section 4.

(3) High computational efficiency

The major advantage of the PUFEM over other methods is that the enrichment process incurs only a small increase in the degrees of freedom (DOFs). In other words, it leads to insignificant increase of number of unknowns. But this slightly incremental computational cost leads to significant improvement in accuracy. In fact, satisfactory solutions can be obtained by limiting the enrichment over only a narrow near-zone of the interface boundary, and leaving the rest un-enriched. By such strategy, the weird behaviour in the near-zone of the singularities is captured by the enriched cover functions, while the far-zones are also well represented with sufficient accuracy. Hence, the penalty of higher computational cost due to the necessity of higher-order numerical integration for the enhanced cover function is limited, and the increase in computational cost is modest.

The main objective of this paper is to present the formulation of an enriched PUFEM for the solution of interface problems. Firstly, it gives a brief review on the general formulation of the PUFEM. What follow are the choices of the enrichment functions and development of different

enrichment schemes. Subsequently, the performance of the present PUFEM is assessed against two benchmark problems.

2. General formulation of PUFEM

Before addressing to the interface issue, a concise review on the PUFEM formulation is necessary. Details of the PUFEM formulation used in this study can be found in references [11].

In the PUFEM, the approximation function $\mathbf{u}(\mathbf{x})$ is expressed in the form

$$\mathbf{u}(\mathbf{x}) = \sum_{i=1}^{n} \mathbf{N}_i(\mathbf{x}) \mathbf{F}_i(\mathbf{x}) \tag{1}$$

In Eqn.1, n is the number of nodal points in the problem domain Ω. The functions $\mathbf{N}_i(\mathbf{x})$ is the partition-of-unity (PU) function associated with node i. $\mathbf{N}_i(\mathbf{x})$ satisfies the following PU conditions:

$$0 \le \mathbf{N}_i(\mathbf{x}) \le 1 \qquad \forall \mathbf{x} \in \Re^N \tag{2a}$$

$$\sum_{i=1}^{n} \mathbf{N}_i(\mathbf{x}) = 1 \qquad \forall \mathbf{x} \in \Omega \tag{2b}$$

In Eqn.2, N is the dimension of the problem. In the PUFEM formulation, the PU function $\mathbf{N}_i(\mathbf{x})$ is simply the standard C^0 FEM shape function. The function $\mathbf{F}_i(\mathbf{x})$ in Eqn.1 is called the *nodal cover function* at node *i*, and it can be expressed as a linear combination of m_i number of *nodal basis (influence) functions* ψ_{ij}, of which each associates with a *generalized nodal value* $\mathbf{a}_{ij}$. That is,

$$\mathbf{F}_i(\mathbf{x}) = \sum_{j=1}^{m_i} \mathbf{a}_{ij} \psi_{ij} \tag{3}$$

Note that $\mathbf{F}_i(\mathbf{x})$ is only defined over the *cover* associates with node i. In the PUFEM, the cover for a given node is simply the union of all the elements joining to that node [11].

By combining Eqn.3 with Eqn.1, the approximation function can be expressed in the form

$$\mathbf{u}(\mathbf{x}) = \sum_{i=1}^{n} \mathbf{N}_i(\mathbf{x}) \sum_{j=1}^{m_i} \mathbf{a}_{ij} \psi_j \tag{4}$$

It should be mentioned that different sets of nodal basis functions can be employed for different covers and this characteristic of the PUFEM results in high flexibility in the formulation.

In practice, two main types of nodal basis functions, namely, *polynomial basis function* and *enriched basis function*, are commonly used in the PUFEM.

Type 1:

The complete polynomial basis functions in 2D is $\{1, x, y, xy, x^2, y^2,\ldots\}$. However, the PU function is C^0 which has the terms $\{x, y, xy\}$ in it. Therefore, the admissible polynomial basis functions have to be reduced to $\{1, x^2, y^2,\ldots\}$. When the order of the basis function is chosen to be 1 (i.e. p=1), the array of the basis function has only the first term (i.e. $m_i = 1$).

Hence, for $m_i=1$:

$$\{\psi_{i1}\}=\{1\} \tag{5a}$$

When the order of the basis function is chosen to be 2 (i.e. p=2), the array has 3 terms (i.e. $m_i=3$) as follows.

$$\{\psi_{i1}, \psi_{i2}, \psi_{i3}\}=\{1, (x-x_i)^2, (y-y_i)^2\} \tag{5b}$$

In Eqn.5b, (x_i, y_i) are the coordinates of node i.

Similarly, when p=3 and 4, the array of basis functions contain 7 and 12 terms respectively. Due to exclusion of the 3 terms $\{x, y, xy\}$, the general relationship between p and m_i is given by

$$m_i = \begin{cases} \dfrac{(p+1)(p+2)}{2} - 2 & \text{for } p = 1 \\ \dfrac{(p+1)(p+2)}{2} - 3 & \text{for } p > 1 \end{cases} \tag{6}$$

The complete array for the cases of p=3 and p=4 can be found in reference [11].

Note that the use of polynomial basis functions is analogous to the *p*-version refinement in the standard FE analysis. Particularly when the order of the basis function is chosen to be 1 (p=1, $m_i=1$) for all nodes, the cover function (Eqn.3) contains only the nodal values $\mathbf{a}_{i1}$, and subsequently the approximation function (Eqn.4) will be exactly the same as in the standard C^0 FE analysis having the nodal variables $\mathbf{u}_i=\mathbf{a}_{i1}$. Obviously, by adopting progressively increasing number of terms m_i in the nodal basis functions, the effect is the same as performing the adaptive *p*-version FE analysis.

Type2:

Enrichment basis functions are usually of asymptotic type, which is excellent in representing the behaviour in the vicinity of a singularity where the derivatives of the approximation functions are

unbounded. Not unexpectedly, it will lead to greater improvement in accuracy. In general, the use of enrichment basis functions is not limited to a single nodal cover (radiating from the singular point). Nodes in near-zone of a singular point can also adopt the same cover function (radiating from the singular point). Of course, the same cover function is not prohibited to be used for nodes in the far-zone where the singularity has diminishing effect. It is worth noting that different cover functions can be used for different nodal covers, in particular where different materials are encountered. Since most asymptotic solutions are only available in polar coordinates (r,θ) radiating from the singular point [1], the enrichment cover functions for an arbitrary node k are usually expressed in the following form

$$\mathbf{F}_k(r,\theta) = \mathbf{a}_{k1} + \sum_{j=2}^{m_k^e} \mathbf{a}_{kj} r^{\beta_j} \mathbf{f}_{kj}(\theta) \tag{7}$$

By comparing Eqn.7 with Eqn.3, the enrichment basis functions, $\boldsymbol{\psi}_{kj}$ are defined as

$$\boldsymbol{\psi}_{kj}(r,\theta) = \begin{cases} 1 & \text{for } j=1 \\ r^{\beta_j}\mathbf{f}_{kj}(\theta) & \text{for } j=2,...,m_k^e \end{cases} \tag{8}$$

In Eqn.7, m_k^e is the total number of terms in the array of the enrichment basis functions, and $\mathbf{f}_{kj}(\theta)$ are smooth trigonometrical functions of θ. Note that β_2 is also known as the *strength of singularity* of the asymptotic solution which is often denoted as λ such that [1, 23]

$$0 \le \beta_2 = \lambda < 1.0 \tag{9a}$$

Hence, the first derivative of the approximation function is proportional to

$$r^{\beta_1 - 1} = \frac{1}{r^{1-\lambda}} \tag{9b}$$

From Eqn.9b, it can be seen that the choice of these asymptotic functions leads to the desired result that the first derivative of the solution is unbounded at the singular point (r=0), and the smaller λ is, the stronger the singular effect is exhibited. In addition, the first term in Eqn.7 is always a constant ($\mathbf{a}_{k1}$). It ensures the rigid-body movement to be represented.

3. Enrichment functions and enrichment schemes for interface problems

3.1 Enriched cover functions for interface problems

Consider a typical interface region (see Fig.1) which consists of two different sub-regions (Ω^I, Ω^{II}) having different materials and three singular points (S_0, S_1 and S_2). The point S_0 is a re-entrant corner point while S_1 and S_2 are singular points at the interface boundary L_1 and L_2 respectively. The asymptotic analytical forms near the interface singular points S_α (α=0, 1, 2) can be expressed as [9]

$$\begin{aligned} \mathbf{u}_\alpha^I(r_\alpha,\theta_\alpha) &= \sum_{j=1}^{\infty} \mathbf{b}_j (r_\alpha)^{\beta_{\alpha j}} \mathbf{f}_{\alpha j}^I(\theta_\alpha) \quad \text{for } (r_\alpha,\theta_\alpha) \in \Omega^I \\ \mathbf{u}_\alpha^{II}(r_\alpha,\theta_\alpha) &= \sum_{j=1}^{\infty} \mathbf{b}_j (r_\alpha)^{\beta_{\alpha j}} \mathbf{f}_{\alpha j}^{II}(\theta_\alpha) \quad \text{for } (r_\alpha,\theta_\alpha) \in \Omega^{II} \end{aligned} \tag{10}$$

In Eqn.10, $\mathbf{b}_j$ are real coefficients. $\mathbf{u}_\alpha^I(r_\alpha,\theta_\alpha)$ and $\mathbf{u}_\alpha^{II}(r_\alpha,\theta_\alpha)$ are the asymptotic forms for the region Ω^I and Ω^{II} respectively. (r_α, θ_α) are the local polar coordinates originated from the singular point S_α (see Fig. 1). $\mathbf{f}_{\alpha j}^I(\theta_\alpha)$ and $\mathbf{f}_{\alpha j}^{II}(\theta_\alpha)$ are smooth functions defined in the regions Ω^I and Ω^{II} respectively. Note that their exact expressions depend on the nature of the physical problem and the corresponding governing equation. The term $\beta_{\alpha 2}$ is equal to λ_α which denotes the strength of singularity at point S_α. That is, (c.f. Eqn.9a)

$$0 \le \beta_{\alpha 2} = \lambda_\alpha < 1.0 \tag{11}$$

By comparing Eqn.7 with Eqn.10, one can easily see that the enrichment basis functions for the cover of the singular point S_α, (α=0, 1, 2) should be defined as (c.f. Eqn. 8)

$$\boldsymbol{\psi}_{\alpha j}(r,\theta) = \begin{cases} (r_\alpha)^{\beta_{\alpha j}} \mathbf{f}_{\alpha j}^I(\theta_\alpha) & \text{for } (r_\alpha,\theta_\alpha) \in \Omega^I \\ (r_\alpha)^{\beta_{\alpha j}} \mathbf{f}_{\alpha j}^{II}(\theta_\alpha) & \text{for } (r_\alpha,\theta_\alpha) \in \Omega^{II} \end{cases} \quad j=2,\ldots,m_\alpha^e \tag{12}$$

Of course, the first term in the array of basis function remains to be 1 (for j=1). This term must be included in order to be able to reflect the rigid-body motion. In Eqn.12, m_α^e is the total number of terms in the array of enriched basis defining the cover of the singular point S_α. It was found [11] that the second term in the enriched basis function $\boldsymbol{\psi}_{\alpha 2}(r,\theta)$ is the most important term in Eqn.12 and the use of $\boldsymbol{\psi}_{\alpha 2}(r,\theta)$ alone will be able to improve the accuracy of the solution tremendously.

Accordingly, only 2 terms (m_α^e =2) are employed in all the numerical examples presented in the next section. As such, the enriched cover function $\mathbf{F}_\alpha(r_\alpha,\theta_\alpha)$ will adopt the following form (c.f. Eqn.7);

$$\mathbf{F}_\alpha(r_\alpha,\theta\alpha)=\begin{cases}\mathbf{a}_{\alpha 1}+\mathbf{a}_{\alpha 2}(r_\alpha)^{\beta_{\alpha 2}}\mathbf{f}^{I}_{\alpha 2}(\theta_\alpha) & \text{for } (r_\alpha,\theta_\alpha)\in\Omega^{I}\\ \mathbf{a}_{\alpha 1}+\mathbf{a}_{\alpha 2}(r_\alpha)^{\beta_{\alpha 2}}\mathbf{f}^{II}_{\alpha 2}(\theta_\alpha) & \text{for } (r_\alpha,\theta_\alpha)\in\Omega^{II}\end{cases} \qquad (13)$$

3.2 Enrichment schemes for interface problems

As mentioned in Section 1, one of the advantages of the PUFEM over many other methods in solving interface problems is its flexibility in implementing the enrichment procedures. In this paper, three different enrichment schemes are presented.

Single-cover enrichment scheme

In the single-cover enrichment scheme, only the cover functions for the singular points are of the enrichment type. Cover functions for other nodes are of the ordinary polynomial type. Consider an arbitrary location in the element bounded by 4 nodes S_0-5-9-1 in Ω^{II} (see Fig.1). It falls within the nodal covers of the four nodes S_0, 5, 9 and 1. Since C^0 PU function is adopted in the present formulation, the approximation function (Eqn.1) for that location is reduced to a sum of those terms only involving N_{s0}, N_5, N_9 and N_1. For the sake of illustration, the enriched cover functions of the singular node S_0 use only 2 terms (m^e_i =2), while the others of polynomial type use 1 term only (p=1, m_i=1). The approximation function over the element can then be written as follows.

$$\mathbf{u}(x)=\mathbf{N}_{S_0}\left[\mathbf{a}_{S_0 1}+\mathbf{a}_{S_0 2}(r_{S_0})^{\beta_{S_0 2}}\mathbf{f}^{II}_{S_0}(\theta_{S_0})\right]+\sum_{i=1,5,9}\mathbf{N}_i(x)a_{i1} \qquad (14a)$$

In the first term of Eqn.14a, the expression within the square bracket corresponds to the enriched nodal cover of node S_0. $\mathbf{N}_i(\mathbf{x})$ (i=S_0, 1, 5, 9) are bilinear shape functions. In this regard, this particular element has one additional degree of freedom ($\mathbf{a}_{S_0 2}$) compared to the un-enriched one.

Similarly, for the element S_0-3-4-5 which is located inside Ω^I, the approximation function $\mathbf{u}(\mathbf{x})$ is given by

$$\mathbf{u}(x)=\mathbf{N}_{S_0}\left[\mathbf{a}_{S_0 1}+\mathbf{a}_{S_0 2}(r_{S_0})^{\beta_{S_0 2}}\mathbf{f}^{I}_{S_0}(\theta_{S_0})\right]+\sum_{i=3,4,5}\mathbf{N}_i(x)a_{i1} \qquad (14b)$$

It is worth noting that this single-cover scheme can be applied to other singular points too.

Multi-cover enrichment scheme

In the multi-cover enrichment scheme, choice of nodal covers to be of enrichment type is not necessary restricted to the singular points. It is arbitrary. Of course, a selection of isolated patches serves no purposes. It is only logical to select a cluster of closely-knitted nodal covers in the near-zone of a singular point, and to adopt the same form of enrichment. For example, nodal covers of nodes S_0, 5, 9 and 1 (see Fig.1) are chosen to be enriched. Their nodal basis functions are all of the same enrichment type (i.e. using 2 terms: $m^e_i = 2$). The approximation function for an arbitrary location inside the element S_0-5-9-1 is as follows.

$$\mathbf{u}(x) = \sum_{i=S_0,1,5,9} \mathbf{N}_i(x)\left[\mathbf{a}_{i1} + \mathbf{a}_{i2}(r_{S_0})^{\beta_{S_0 2}} \mathbf{f}^{II}_{S_0}(\theta_{S_0})\right] \qquad (15)$$

In this case, that particular element has 4 additional degrees of freedom (i.e. $\mathbf{a}_{i2}$, i=S_0, 5, 9 and 1) compared to the un-enriched one (p=1).

Interface multi-cover enrichment scheme

This scheme is a special case of the multi-cover enrichment scheme. The nodal covers of all nodes lying on the interface boundary (L_1 and L_2 in Fig.1) are chosen to be of enrichment type, while others are of polynomial type. Consider the element 1-9-10-6 next to the interface boundary. Nodes 1 and 6 lie on the interface, and their nodal covers are of enrichment type (i.e. using 2 terms, $m^e_i = 2$). Nodes 9 and 10 do not lie on the interface, and their nodal covers are of the ordinary polynomial type (i.e. using 1 term: p=1, m_i=1). The approximation function for an arbitrary location inside the element 1-9-10-6 is as follows.

$$\begin{aligned}\mathbf{u}(x) = {} & \mathbf{N}_1(x)\left[\mathbf{a}_{S_0 1} + \mathbf{a}_{S_0 2}(r_{S_0})^{\beta_{S_0 2}} \mathbf{f}^{II}_{S_0}(\theta_{S_0})\right] + \mathbf{N}_6(x)\left[\mathbf{a}_{S_1 1} + \mathbf{a}_{S_1 2}(r_{S_1})^{\beta_{S_1 2}} \mathbf{f}^{II}_{S_1}(\theta_{S_1})\right] + \\ & \mathbf{N}_9(x)\mathbf{a}_{91} + \mathbf{N}_{10}(x)\mathbf{a}_{10,1}\end{aligned} \qquad (16)$$

Note that in Eqn. 16, the enrichment basis functions for nodes 1 and 6 are different. Since there are two singular points nearby, the choice is arbitrary. Of course, it is logical to adopt the enrichment form of the nearest singular nodal cover. For node 1, distance-wise $|S_0 1| < |S_1 1|$ and the nearest is node S_0. Therefore, its nodal cover functions are kept in line with node S_0. For node

6, distance-wise $|S_1 6| < |S_0 6|$ and the nearest is node S_1. Hence, its nodal cover functions are kept in line with node S_1.

4. Numerical examples

In this section, two elliptic interface problems are solved by using the PUFEM described in Sections 2 and 3. Formation of algebraic equation system is similar to the standard FEM procedure and the contributions to the global stiffness matrix are computed in an element-by-element manner. In all the computations, the standard 4-node bilinear quadrilateral FE shape functions are used as the PU functions. In both examples, three different enrichment schemes (single-, multi- and interface-multi-cover) are applied to obtain solutions, and their effect on the accuracy of the solution are compared. Their performances are also compared with the results obtained by standard uniform *h*-refinement FE analysis. In addition, in Example 2 where more than one singular point exists, the effect of enrichment over different singular zones on the accuracy of the solution is also investigated.

4.1 Example 1: Laplace equation defined over an L-shaped domain

The Laplace equation with one interface defined over an L-shaped domain (see Fig.2) is taken as the first example. The governing differential equation is given by [24]

$$\begin{aligned} -\nabla\cdot(q_1\nabla u) &= Q_1 \quad \text{in } \Omega^{I} \\ -\nabla\cdot(q_2\nabla u) &= Q_2 \quad \text{in } \Omega^{II} \end{aligned} \tag{17a}$$

$$u=0 \quad \text{on } \partial\Omega \tag{17b}$$

In Eqn.17, $\Omega=\Omega^{I}\cap\Omega^{II}$ with $\Omega^{I}=[-1,0]\times[-1,1]$ and $\Omega^{II}=[0,1]\times[0,1]$ (see Fig. 2). The line of interface discontinuity (related to the coefficients q_1 and q_2 in Eqn.17a) is a straight line linking the points (0,0) and (0,1). The values of Q_1 and Q_2 on the RHS of Eqn.17a are defined as

$$\begin{aligned} Q_1 = {} & q_1 2r^{\beta}(2-r^2)\frac{\sin(3\pi\beta/2-\beta\theta)}{2\cos(\pi\beta/2)} + \\ & 4q_1\beta r^{\beta-1}\left[x(1-y^2)\frac{\sin(3\pi\beta/2-(\beta-1)\theta)}{2\cos(\pi\beta/2)} - y(1-x^2)\frac{\cos(3\pi\beta/2-(\beta-1)\theta)}{2\cos(\pi\beta/2)}\right] \end{aligned} \tag{18a}$$

$$Q_2 = q_2 2r^{\beta}(2-r^2)\sin(\beta\theta) + 4q_2\beta r^{\beta-1}\left[x(1-y^2)\sin((\beta-1)\theta) + y(1-x^2)\cos((\beta-1)\theta)\right] \quad (18b)$$

such that the exact solution u^{ex} is given by

$$u^{ex}(x,y) = \begin{cases} (1-x^2)(1-y^2)r^{\beta}\sin(\beta\theta) & \text{for } x > 0 \\ (1-x^2)(1-y^2)r^{\beta}\dfrac{\sin(\beta(3\pi/2-\theta))}{2\cos(\beta\pi/2)} & \text{for } x \le 0 \end{cases} \quad (19)$$

In Eqns.18 and 19, β is the strength of singularity, which is a function of the ratio q_1/q_2 and is given by

$$\beta = \frac{2}{\pi}\tan^{-1}\left(\sqrt{1+\frac{2q_2}{q_1}}\right) \quad (20)$$

The singular point of this problem is located at the point S_0 where r=0 with the first derivative of the solution, $u^{ex'}$, unbounded and of the order $O(1/r^{(1-\beta)})$. It can be seen from Eqn.20 that the higher the ratio q_1/q_2 grows, the stronger the singularity at the point S_0 exhibits.

Based on the enriched PUFEM formulation mentioned above, Eqn.19 can be included in the enriched array of basis functions such that

$$\psi_1(x,y) = \begin{cases} (1-x^2)(1-y^2)r^{\beta}\sin(\beta\theta) & \text{for } x > 0 \\ (1-x^2)(1-y^2)r^{\beta}\dfrac{\sin(\beta(3\pi/2-\theta))}{2\cos(\beta\pi/2)} & \text{for } x \le 0 \end{cases} \quad (21)$$

The performance of this enriched formulation and the accuracy is judged from the energy norm of solution error $\|e_u\|_e$, which is defined as

$$\|e_u\|_e = \|u^{ex} - u^{PU}\|, \quad \|v\|_e = \left(\int_{\Omega}(\nabla v \cdot \nabla v)d\Omega\right)^{1/2} \quad (22a)$$

and the relative error of solution η, which is defined as

$$\eta = \frac{\|e_u\|_e}{\|u^{ex}\|_e} \times 100\% \quad (22)$$

In Eqn.22, u^{ex} and u^{PU} denote respectively the exact solution and the solution obtained from the present PUFEM formulation.

Four different meshes (Meshes 1 to 4) of 4-node finite elements (Fig. 3) generated by uniform *h*-refinement are used in the numerical study. The 5×5 Gauss integration scheme are used for the integration of the global equation system. The above-mentioned three different enrichment schemes are applied. Results are compared with those obtained by standard FE analysis (i.e. no enrichment and p=1). In the single-cover enrichment scheme, only the nodal cover of the singular point S_0 is enriched (using 2 terms: $m^e_{S_0}=2$). In the multi-cover enrichment scheme, nodal covers of all nodes falling in the hatched region (see Fig. 3) are chosen to be of the enrichment type (using 2 terms: $m^e_{S_0}=2$). In the interface-multi-cover enrichment scheme, nodal covers of all nodes lying on the line (S_0A) are enriched (using 2 terms: $m^e_{S_0}=2$). All other nodal covers are of polynomial type (p=1). The convergence rates of solutions are investigated using the following formula.

$$R(\eta)=\frac{\log(\eta_i/\eta_{i+1})}{\log(NDOF_{i+1}/NDOF_i)} \qquad (23)$$

In Eqn. 23, η_i denotes the relative error obtained from the i^{th} mesh (i=1, 2, 3, 4). $NDOF_i$ is the total number of degrees of freedom in the i^{th}-mesh analysis. In order to study the performance of the enriched PUFEM formulation against the strength of singularity (β), three pairs of different values of q_1/q_2 corresponding to β=0.5032, 0.6667 and 0.9052 (Table 1) are used. Totally, 36 combinations (4 meshes × 3 enrichment schemes × 3 β values) of enriched PUFEM analyses and 4 non-enriched FE analyses are carried out. Note that if standard FEM is used to solve this problem, the theoretical rate of convergence for an *h*- refinement will equal to β.

The results obtained for β=0.5032, 0.6667 and 0.9552 under different enrichment schemes are listed in Tables 2, 3 and 4 respectively. For easy visualization, the results are also plotted (in logarithmic scale) in Figs. 4 to 6. From Tables 2 to 4 and Fig. 4 to 6, the following conclusions can be drawn.

(1) For different values of q_1/q_2 (hence different values of β), the use of different enrichment schemes all leaded to improvements in accuracy. However, the improvement diminishes as β increases. It is expected as in this problem, a higher value of β implies a weaker

singularity at the point S_0. The problem becomes relatively easy to solve and therefore, the impact of the enrichment formulation on the accuracy of the solution diminishes.

(2) For different ratios (β), the multi-cover enrichment scheme yields the most accurate solutions. The interface-multi-cover scheme appears to have slightly better performance than the single-cover scheme. However, the differentials among them are relatively small when compared to their improvement over the no-enrichment results (FE analysis). They all show significant improvement in the accuracy of solution. On the other hand, in terms of efficiency against increase of DOF, the single enrichment scheme is the winner because it attains the achievement by merely increasing one DOF.

(3) While all the enrichment schemes show great improvements in the accuracy of solution, no significant improvement in convergence rate is observed as compared to the no-enrichment (FE) analysis. It agrees with the observations reported in previous study of PUFEM [11]. It leads to a logical deduction that improved convergence rate can only be achieved when the enriched PUFEM is used in conjunction with *p*-version refinement.

4.2 Example 2: Elliptic problem with three singular points

In the second example, a self-adjoint elliptic problem with three singular points is considered. The problem domain is a square of size 4×4 (see Fig.7) consisting of two sub-regions (Ω^{I} and Ω^{II}) and two interface boundaries (L_1 and L_2). The governing differential equation and the boundary conditions are given by

$$\nabla \cdot (q\nabla u) = 0 \quad \text{in } \Omega = \Omega^{I} \cup \Omega^{II} \tag{24a}$$

$$u=0 \quad \text{on } \Gamma_1 \quad \text{and} \quad q\frac{\partial u}{\partial \mathbf{n}} = g \quad \text{on } \Gamma - \Gamma_1 \tag{24b}$$

In Eqn.24, Γ is the boundary of Ω such that $\Gamma=\Gamma_1\cup\Gamma_2\cup\Gamma_3\cup\Gamma_4$. $\mathbf{n}$ is the outward normal vector along Γ. The coefficients q and g are defined as

$$q = \begin{cases} 30 & \text{in } \Omega^{I} \\ 1 & \text{in } \Omega^{II} \end{cases} \quad \text{and} \quad g = \begin{cases} 1 & \text{in } \Gamma_3 \\ 0 & \text{in } \Gamma_2 \cup \Gamma_4 \end{cases} \tag{25}$$

Three singular points $S_0(0,0)$ $S_1(2,-2)$ and $S_2(2,2)$ are present. The leading terms of the asymptotic solutions (Eqn.10) at these three singular points are as follows [3].

For S_0:

$$u^{I}(r_{s_0},\theta_{s_0}) = b_{S_0}\left(\frac{\sin(\beta_{s_0}\pi)(62\cos(\beta_{s_0}\pi)+2)}{62\cos^2(\beta_{s_0}\pi)+2\cos(\beta_{s_0}\pi)-31}\sin(\beta_{s_0}\pi)+\cos(\beta_{s_0}\pi)\right)r^{\beta_{s_0}}$$

$$u^{II}(r_{s_0},\theta_{s_0}) = b_{S_0}\left(\frac{-60\sin(\beta_{s_0}\pi)\sin(\beta_{s_0}\theta_{s_0})+(2\cos(\beta_{s_0}\pi)+31)\cos(\beta_{s_0}\theta_{s_0})}{62\cos^2(\beta_{s_0}\pi)+2\cos(\beta_{s_0}\pi)-31}\right)r^{\beta_{s_0}} \quad (26a)$$

$$\beta_{s_0} = 0.609135$$

For S_i, i=1,2:

$$u^{I}(r_{s_i},\theta_{s_i}) = b_{S_i}(-1)^{i}(\tan(\beta_{S_i}\pi/2)-\tan(\beta_{S_i}\pi/4))\cos(\beta_{S_i}\theta_{S_i})r^{\beta_{S_i}}$$

$$u^{II}(r_{s_i},\theta_{s_i}) = b_{S_i}\left(\sin(\beta_{S_i}\theta_{S_i})+(-1)^{i}\tan(\beta_{S_i}\pi/2)\cos(\beta_{S_i}\theta_{S_i})\right)r^{\beta_{S_i}} \quad (26b)$$

$$\beta_{S_i} = 0.229928$$

Since $\beta_{S_0} > \beta_{S_1} (=\beta_{S_2})$, the strength of singularity at points S_1 and S_2 are stronger than that at S_0. We can anticipate that error of the approximation solution near the points S_1 and S_2 will be more severe.

In this example, both uniform *h*- and *p*-refinements are carried out in conjunction with different enrichment schemes. In all cases, two-term enrichment basis functions ($m_i^e=2$) are used. It consists of a constant (the first term) and the leading term of the asymptotic solution (Eqn.26).

In the uniform *h*-refinement analyses, four uniformly refined meshes are used (see Fig.8). In addition to the no-enrichment (FE) analysis, the *h*-refinement analyses are carried out in junction with the following five different enrichment schemes.

(1) *h-e1*: Single-cover enrichments at nodes S_0, S_1 and S_2

(2) *h-e2*: Single-cover enrichment at node S_0 only

(3) *h-e3*: Single-cover enrichment at node S_1 only

(4) *h-e4*: Interface-multi-cover enrichment at nodes on line L_1 only

(5) *h-e5*: Interface-multi-cover enrichments at nodes on lines L_1 and L_2

In the uniform *p*-refinement analyses, the mesh (see Fig.9) consisting 16 elements is used. Note that the *p*-refinements are performed over the non-enriched nodal covers only, using 3 different orders of polynomial-type cover functions (p=1, 2, 3). The *p*-refinement analyses are carried out in junction with the following four different enrichment schemes.

(1) *p-e1*: Single-cover enrichments at nodes S_0, S_1 and S_2

(2) *p-e2*: Single-cover enrichment at node S_0 only

(3) *p-e3*: Single-cover enrichment at node S_1 only

(4) *p-e4*: Single-cover enrichments at node S_1 and S_2

Note that for the two lower order *p*-refinements (*p*=1, 2), 5×5 Gauss integration scheme is used while 10×10 Gauss integration scheme is used for *p*=3.

In this example, unlike the case in Example 1, no closed form solution is available. As such, the resulting energy norm obtained through Eqn.22a from the highest order *p*-refinement FE analysis [9] is used as the benchmark (or 'exact') solution, $\left\|u^{ex}\right\|_{\mathbf{e}}$=0.8682663819654824. As the model problem is self-adjoint, provides that the squares of the energy norms of the benchmark solution, $\left\|u^{ex}\right\|_e^2$, and the PU solution, $\left\|u^{PU}\right\|_e^2$, are computed accurately using an adequate numerical integration rule, it is well known that the error in the squares of energy norms , $\left\|u^{ex}\right\|_e^2 - \left\|u^{PU}\right\|_e^2$ is a good approximation to the square of the energy norm of the error, $\left\|u^{ex} - u^{PU}\right\|_e^2$. Accordingly, the performances of different schemes are assessed by the relative error in energy norm η_e which is defined as

$$\eta_e = \frac{\sqrt{\left|\left\|u^{ex}\right\|_e^2 - \left\|u^{PU}\right\|_e^2\right|}}{\left\|u^{ex}\right\|_e} \times 100\% \qquad (27)$$

Subsequently, the convergence rate of solutions $R(\eta_e)$ can be investigated using Eqn.23 by replacing η by η_e.

The results obtained from the uniform *h*- and *p*-refinements are listed in Tables 5 and 6 respectively. For easy visualization, the trends of relative error norm η_e under different enrichment schemes are plotted against the total DOF in Figs.10 and 11 for *h*- and *p*-refinements respectively. From Tables 5 and 6 and Figs.10 and 11, the following conclusions can be drawn.

(1) In the *h*-refinements, use of any (expect the *h-e2*) enrichment scheme leads to significant reduction in the relative error η_e. Particularly, the interface-multi-cover scheme *h-e5* yields the most accurate result. On the other hand, in terms the efficiency, the winner is

the *h-e1* scheme, in which single-cover enrichments are used at all singular points S_0, S_1 and S_2 only. Improved accuracy of solution is achieved by adding only 3 DOF. In this logic, the second on the efficient list goes to other single-cover enrichment schemes. Examining the strength of singularity at the three singular points reveals that the strengths at S_1 and S_2 are both stronger than that at S_0. Hence not unexpectedly, the *h-e3* scheme having singe-cover enrichment at S_1 (or S_2) performs better than the *h-e2* scheme which has singe-cover enrichment at S_0. Lastly, the *h-e4* scheme having interface-multi-cover enrichment over the line L_1 was found yielding almost identical results as the single-cover enrichment scheme *h-e3*. It shows that single-cover enrichment scheme (*h-e3*) is not only more efficient than the interface-multi-cover enrichment scheme (*h-e4*), but also yields same order of accurate solution. Regarding the convergence rate of the solution, similar conclusion is observed as in Example 1 that no significantly improvement can be seen through *h*-refinements.

(2) In the *p*-refinements, a general trend of producing solutions of reduced error than the *h*-refinements is observed. To differentiate the performance of different *p*-refinement schemes, similar conclusion can be drawn as that for the *h*-refinements. Use of the highest order of *p*-refinement in conjunction single-cover enrichments at all singular points (*p-e1* scheme) yields the most accurate solution. Enriching the nodal covers at both singular points S_1 and S_2 (*p-e4* scheme) is more effective than just enriching the nodal cover at S_0 (*p-e2* scheme) or S_1 (*p-e3* scheme) alone. Regarding the convergence rate of the solution, increasing order of *p* in conjunction any enrichment schemes shows improved convergence rate. This observation agrees with findings obtained in the pervious studies [10, 11].

5. Conclusions

Formulation and applications of the enriched PUFEM for the solution of singular interface problems are illustrated. Available asymptotic solutions for the near-zone of a singular point are included in the enhanced array of basis functions. It leads to solutions of much improved accuracy. Implementation of the enrichment procedure is simple and flexible. Different enrichment schemes can be incorporated with the same procedure. It demands no special integration technique. The effectiveness of different enrichment schemes in conjunction with

various uniform *h*- and *p*-refinements are demonstrated in the numerical examples. In general, any enrichment scheme in tandem with either refinement can greatly enhance the quality of the solution. Particularly, using merely single-cover enrichments at all singular points turns out to be the most effective. It only incurs incremental increase of computational cost but yields solutions of significantly improved accuracy. Regarding the convergence rate, no significant improvement is observed in all uniform *h*-refinements in conjunction with any enrichment schemes. But improved convergence rates are often observed in increasing order of *p*-refinements in conjunction any enrichment scheme.

Reference

1. B. Szabo and I. Babuska, "Finite element analysis", John Wiley & Sons, Inc. 1991

2. I. Babuska and B. Guo, "Regularity of the solutions of elliptic problem with piecewise analytic data, part I: boundary values problems or linear elliptic equation of second order", SIAM J. Math. Anal. **19**, 172-203 (1988)

3. I. Babuska and B. Guo, "On the regularity of elasticity problem with piecewise analytic data", Advances in Applied Mathematics, **14**, 307-347 (1993)

4. O. C. Zienkiewicz and J. Z. Zhu, The three R's of engineering analysis and error estimation and adaptivity, *Comput. Methods Appl. Mech. Engrg.,* **82,** 95-113 (1990)

5. O. C. Zienkiewicz and J. Z. Zhu, Adaptivity and mesh generation, *Int. J. Numer. Methods Engrg.,* **32,** 783-810 (1991)

6. C. K. Lee and S. H. Lo, An automatic adaptive refinement finite element procedure for 2D elastostatic analysis, *Int. J. Numer. Methods Engrg.,* **35,** 1967-1989 (1992)

7. T. Strouboulis and K. A. Haque, Recent experiences with error estimation and adaptivity, Part I: Review of error estimators for scalar elliptic problems, *Comput. Methods Appl. Mech. Engrg.,* **97,** 399-436 (1992)

8. T. Strouboulis and K. A. Haque, Recent experiences with error estimation and adaptivity, Part II: Error estimation for *h*-adaptive approximations on grids of triangles and quadrilaterals, *Comput. Methods Appl. Mech. Engrg.,* **100,** 359-430 (1992)

9. H. S. Oh and I Babuska, "The *h-p* version of the finite element method for problems with interface", *Int. J. Numer. Methods Engrg.,* **37,** 1741-1762 (1994)

10. M. K. Melenk and I. Babuska, "The partition of unity finite element method: basic theory and application", *Comput. Methods Appl. Mech. Engrg.,* **139,** 289-314 (1996)

11. X. Liu, C. K. Lee and S. C. Fan, "On using enriched function in the Partition-of-unity method for singular boundary-value problems", *Computational Mechanics*, **29**, 212-225 (2002)

12. I. Babuska and J. M. Melenk, "The partition of unity method", *Int. J. Numer. Methods Engrg.,* **45,** 727-158 (1997)

13. C. A. Duarte and J. T. Oden, "An H-p adaptive method using clouds", *Comput. Methods Appl. Mech. Engrg.,* **139,** 237-262 (1996)

14. T. Strouboulis, I. Babuska and K. Copps, "The design and analysis of the generalized finite element method", *Comput. Methods Appl. Mech. Engrg.,* **181,** 43-69 (2000)

15. T. Strouboulis, K. Copps and I. Babuska, "The generalized finite element method: An example of its implementation and illustration of its performance", *Int. J. Numer. Methods Engrg.,* **47,** 1401-1417 (2000)

16. T. Strouboulis, K. Copps and I. Babuska, "The generalized finite element method", *Comput. Methods Appl. Mech. Engrg.,* **190,** 4081-4193 (2001)

17. T. Belytschko, T. Black, "Elastic crack growth in finite elements with minimal remeshing", *Int. J. Numer. Methods Engrg.,* **45,** 601-620 (1999)

18. N. Moes, J. Dolbow and T. Belytschko, "A finite element method for crack growth without remeshing", *Int. J. Numer. Methods Engrg.,* **46,** 131-150 (1999)

19. C. Daux, J. Dolbow, N. Sukumar and T. Belytschko, "Arbitrary cracks and holes with the extended finite element method", *Int. J. Numer. Methods Engrg.,* **48,** 1741-1760 (2000)

20. Y. Y. Lu, T. Belytschko and L. Gu, A new implementation of the element free Galerkin method, *Comput. Methods Appl. Mech. Engrg.,* **113,** 397-414 (1994)

21. T. Belytschko, L. Gu and Y. Y. Lu, "Fracture and crack growth by element free Galerkin methods", Model. Simul. Material Science. Engrg., **2**, 519-534 (1994)

22. Fleming, M. Chu, Y A. Moran, B. Belytschko, T. Enriched element-free Galerkin methods for crack tip fields, *Int. J. Numer. Methods Engrg.,* **40,** 1483-1504 (1997)

23 I. Babuska and B. A. Szabo, On the rates of convergence of the finite element method, *Int. J. Numer. Methods Engrg.,* **18,** 323-341 (1982)

24. B. Heinrich and S. Nicaise. "Nitsche mortar finite element method for transmission problems with singularities", preprint SFB 393/01-10, TU Chemnitz, 2001

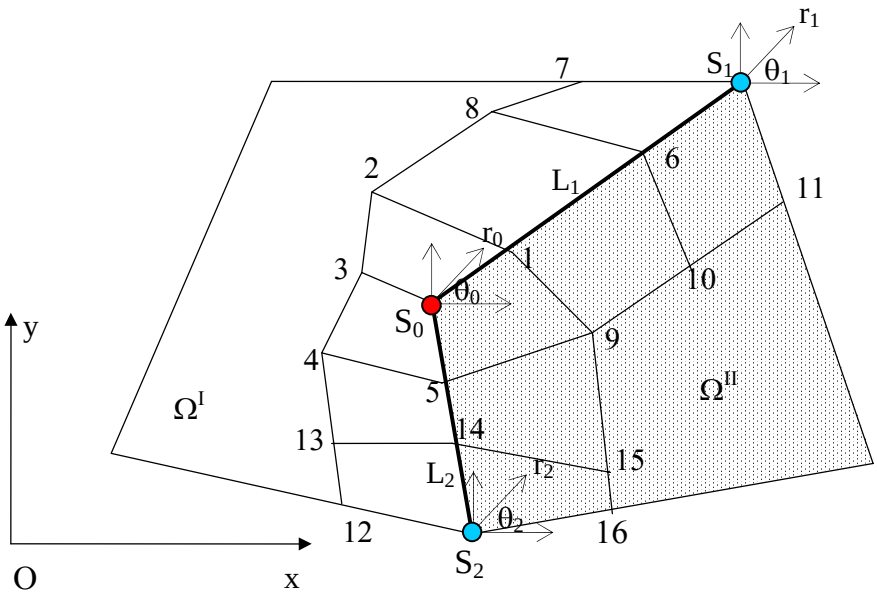

Fig.1 Interface problem having two sub-domains (Ω^I, Ω^{II}) and three singular points (S_0, S_1 and S_2)

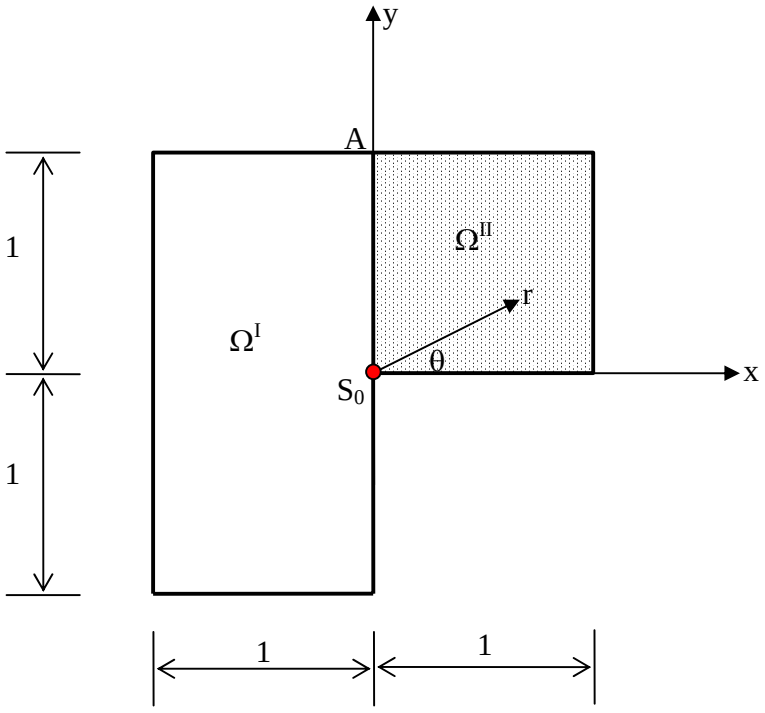

Fig.2 Example 1: An L-shaped domain with one interface boundary

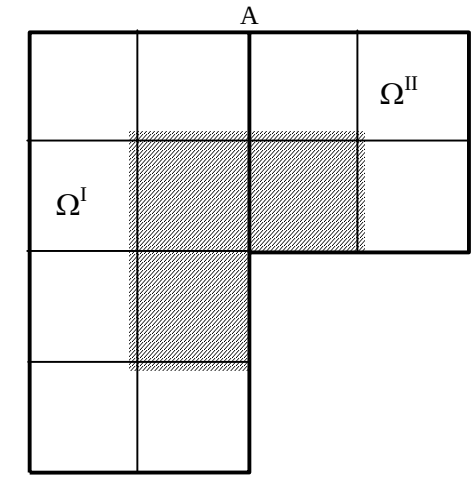

Region in which nodal covers of nodes inside are enriched during multi-enrichment

(a) Mesh 1

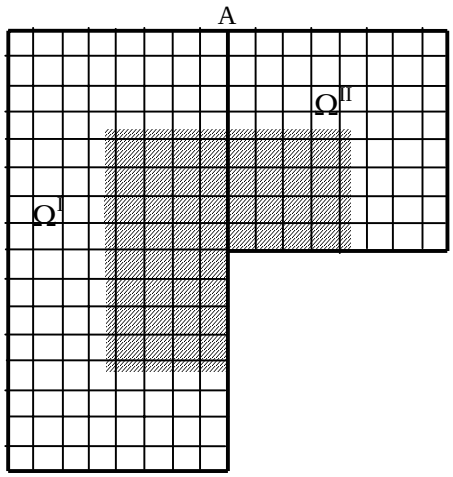

Region in which nodal covers of nodes inside are enriched during multi-enrichment

(c) Mesh 3

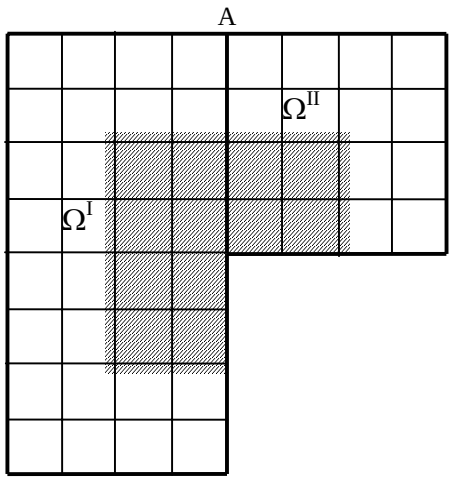

Region in which nodal covers of nodes inside are enriched during multi-enrichment

(b) Mesh 2

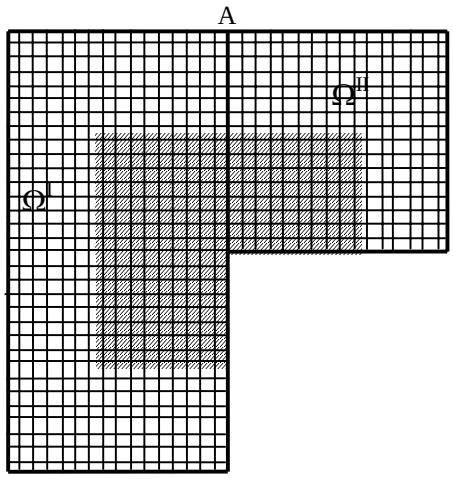

Region in which nodal covers of nodes inside are enriched during multi-enrichment

(d) Mesh 4

Fig.3 Uniform *h*-refinement for Example 1

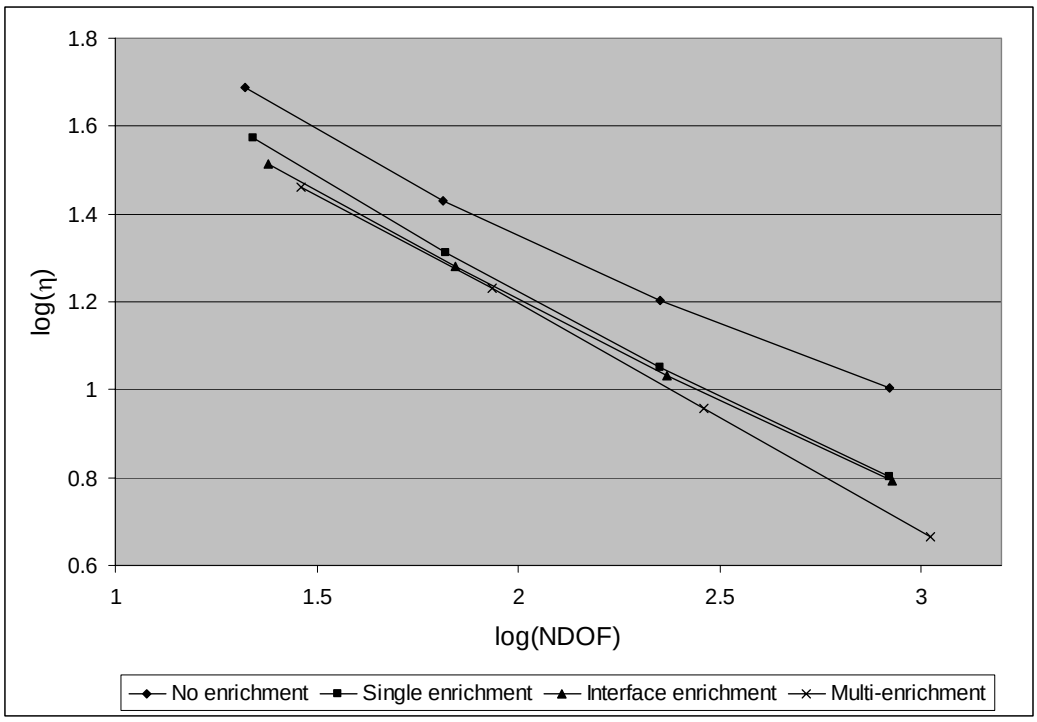

Fig.4 Rate of convergence of Example 1 (q_1=100.0, q_2=1.0, β=0.5032)

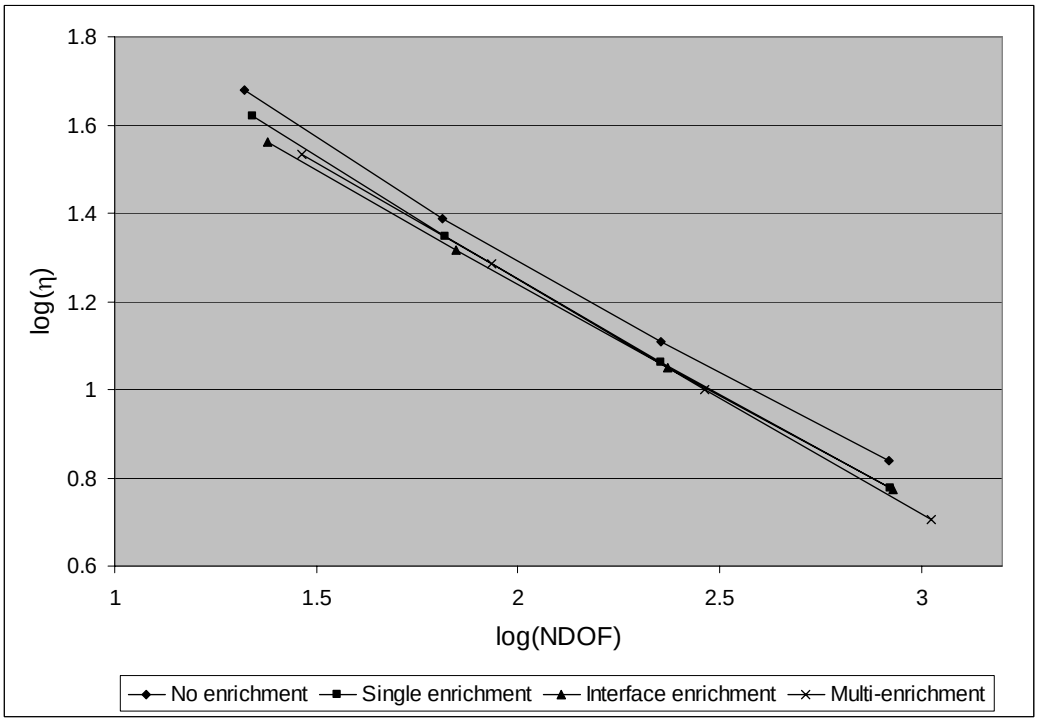

Fig.5 Rate of convergence of Example 1 (q_1=1.0, q_2=1.0, β=0.6667)

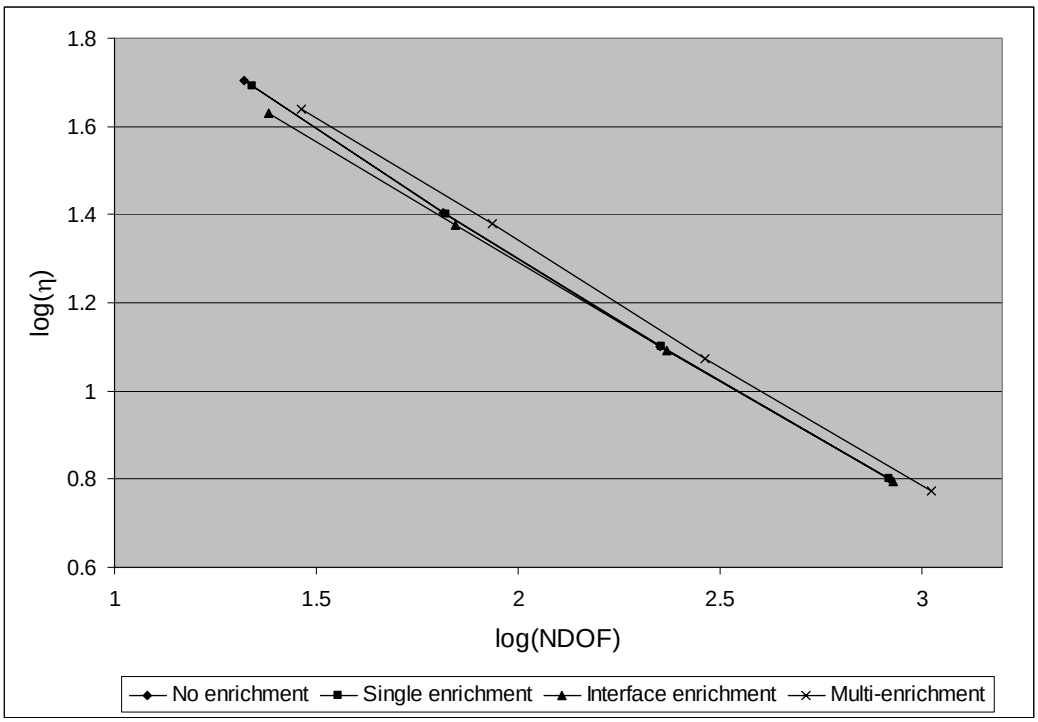

Fig.6 Rate of convergence of Example 1 (q_1=1.0, q_2=1.0, β=0.9552)

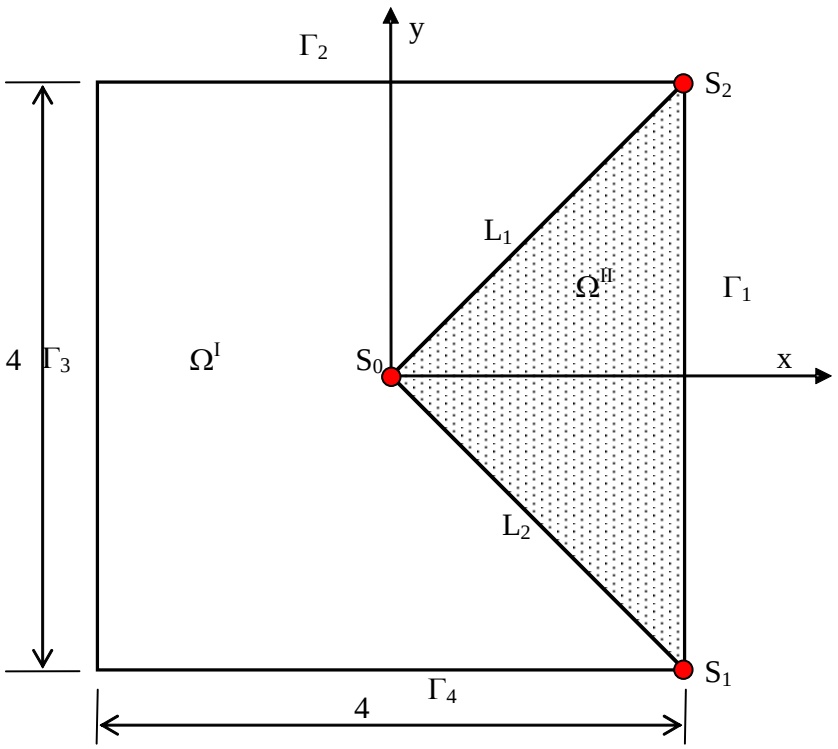

Fig.7 Example 2: An elliptic problem having three singular points

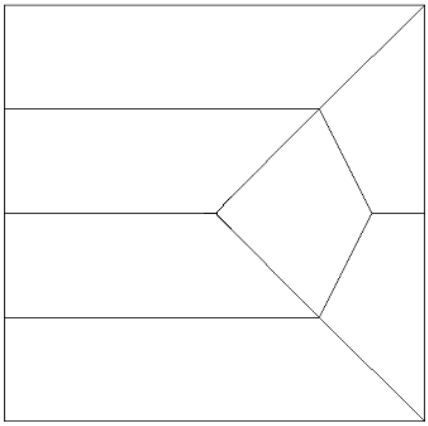

(a) Mesh 1

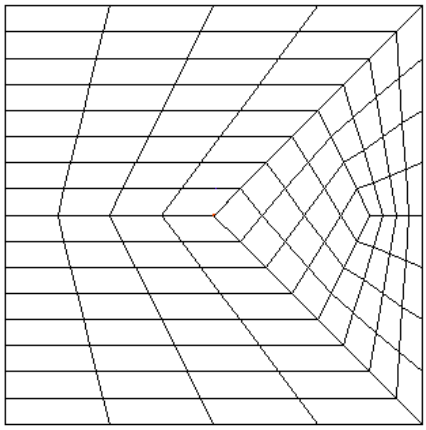

(c) Mesh 3

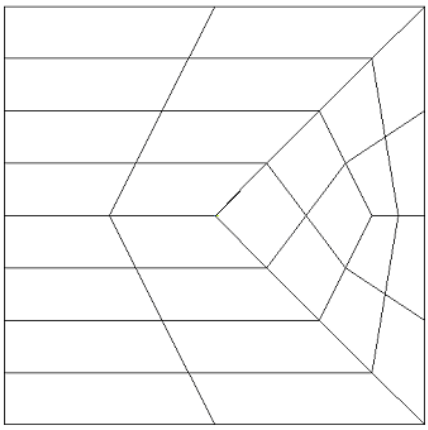

(b) Mesh 2

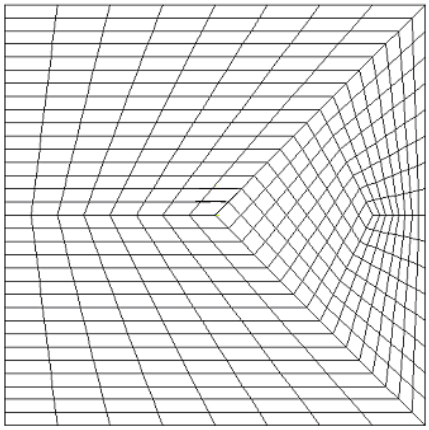

(d) Mesh 3

Fig.8 Uniform *h*-refinement for Example 2

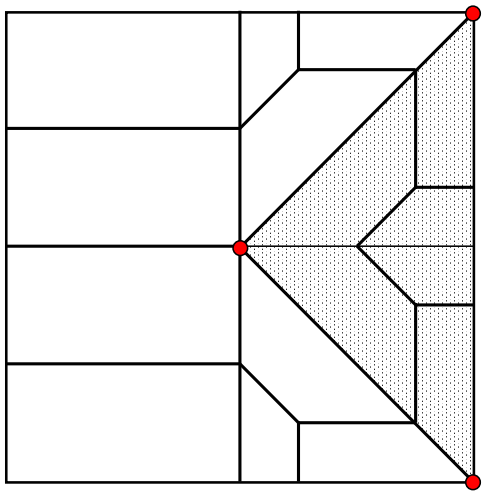

Fig.9 Mesh for *p*-refinement for Example 2

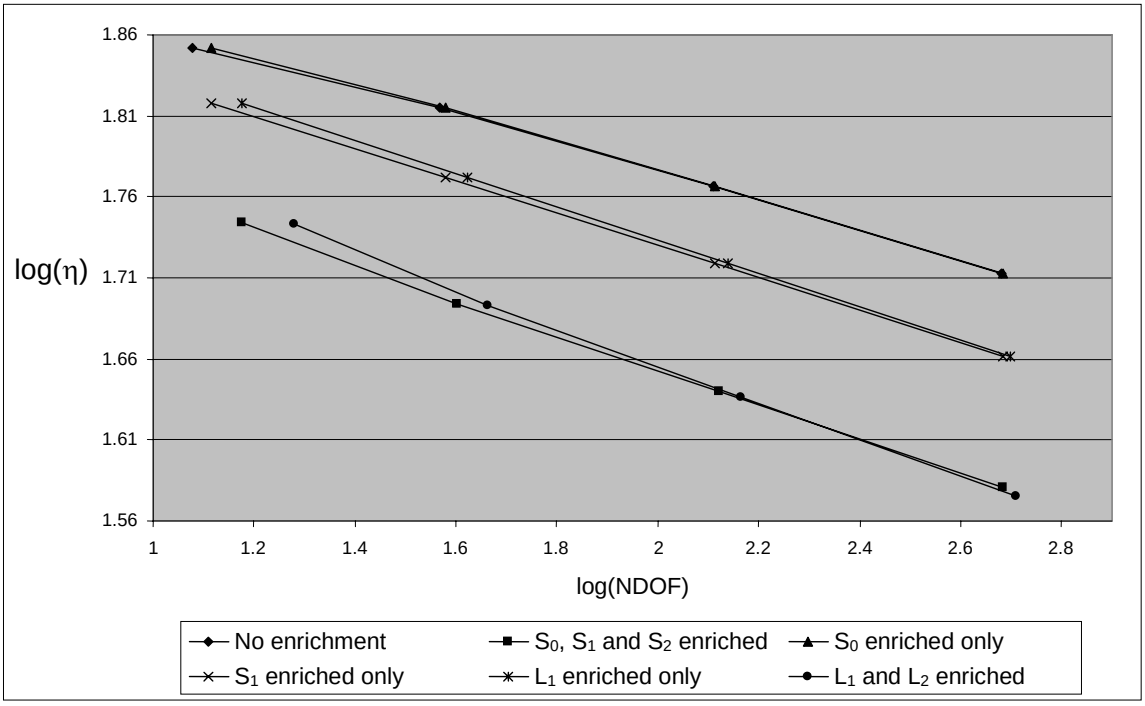

Fig.10 Rate of convergence of Example 2 (*h*-refinement)

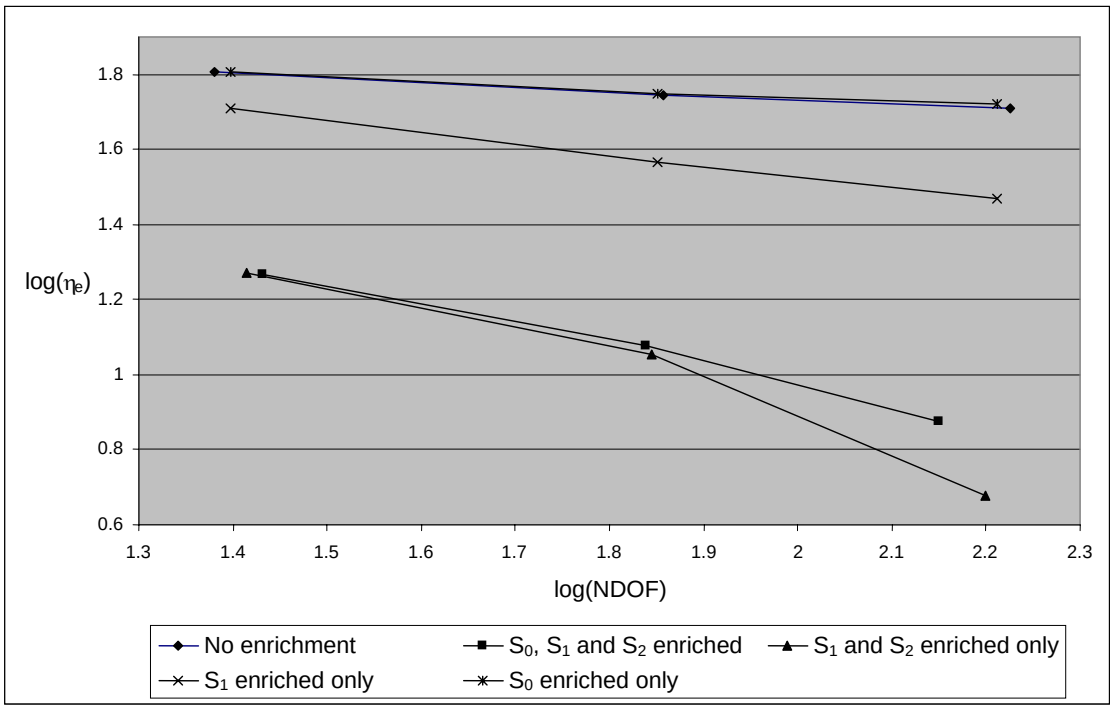

Fig.11 Rate of convergence of Example 2 (*p*-refinement)

Table 1. Values of q_1 and q_2 used in Example 1

q_1	q_2	β
100	1	0.5032
1	1	0.6667
1	100	0.9552

Table 2. Results of Example 1 (q_1=100.0, q_2=1.0, β=0.5032)

No enrichment			
Mesh	DOF	η	R(η)
1	21	48.87	--
2	65	26.92	0.53
3	225	16.00	0.42
4	833	10.10	0.35
Single enrichment			
Mesh	DOF	η	R(η)
1	22	37.48	--
2	66	20.47	0.55
3	226	11.23	0.49
4	834	6.36	0.44
Interface enrichment			
Mesh	DOF	η	R(η)
1	24	32.71	--
2	70	19.07	0.51
3	234	10.79	0.47
4	850	6.19	0.43
Multi-enrichment			
Mesh	DOF	η	R(η)
1	29	28.97	--
2	86	17.06	0.49
3	290	9.10	0.52
4	1058	4.63	0.52

Table 3. Results of Example 1 (q_1=1.0, q_2=1.0, β=0.6667)

No enrichment			
Mesh	DOF	η	R(η)
1	21	47.84	--
2	65	24.42	0.60
3	225	12.82	0.52
4	833	6.90	0.47
Single enrichment			
Mesh	DOF	η	R(η)
1	22	41.81	--
2	66	22.21	0.58
3	226	11.53	0.53
4	834	6.00	0.50
Interface enrichment			
Mesh	DOF	η	R(η)
1	24	36.32	--
2	70	20.75	0.52
3	234	11.20	0.51
4	850	5.92	0.49
Multi-enrichment			
Mesh	DOF	η	R(η)
1	29	34.04	--
2	86	19.34	0.52
3	290	10.03	0.54
4	1058	5.08	0.53

Table 4. Results of Example 1 (q_1=1.0, q_2=100.0, β=0.9552)

No enrichment			
Mesh	DOF	η	R(η)
1	21	50.54	--
2	65	25.28	0.61
3	225	12.64	0.56
4	833	6.32	0.53
Single enrichment			
Mesh	DOF	η	R(η)
1	22	49.05	--
2	66	25.18	0.61
3	226	12.63	0.56
4	834	6.32	0.53
Interface enrichment			
Mesh	DOF	η	R(η)
1	24	42.78	--
2	70	23.76	0.55
3	234	12.31	0.55
4	850	6.25	0.53
Multi-enrichment			
Mesh	DOF	η	R(η)
1	29	43.67	--
2	86	23.93	0.55
3	290	11.83	0.58
4	1058	5.95	0.53

Table 5. Results of Example 2 (*h*-refinement)

No enrichment			
Mesh	DOF	η_e	$R(\eta_e)$
1	12	71.12	--
2	37	65.39	0.075
3	129	58.46	0.090
4	481	51.64	0.094
S_0, S_1 and S_2 enriched			
Mesh	DOF	η_e	$R(\eta_e)$
1	15	55.43	--
2	40	49.40	0.117
3	132	43.61	0.104
4	484	38.11	0.101
S_0 enriched only			
Mesh	DOF	η_e	$R(\eta_e)$
1	13	71.04	--
2	38	65.36	0.078
3	130	58.45	0.091
4	482	51.64	0.095
S_1 enriched only			
Mesh	DOF	η_e	$R(\eta_e)$
1	13	65.77	--
2	38	59.19	0.098
3	130	52.37	0.100
4	482	45.90	0.101
L_1 enriched only			
Mesh	DOF	η_e	$R(\eta_e)$
1	15	65.67	--
2	42	59.19	0.101
3	138	52.35	0.103
4	498	45.87	0.103
L_1 and L_2 enriched			
Mesh	DOF	η_e	$R(\eta_e)$
1	19	55.41	--
2	46	49.26	0.133
3	146	43.27	0.112
4	514	37.58	0.112

Table 6. Results of Example 2 (*p*-refinement)

No enrichment			
p	DOF	η_e	$R(\eta_e)$
1	24	64.05	--
2	72	55.71	0.13
3	168	51.27	0.098
S_0, S_1 and S_2 enriched			
p	DOF	η_e	$R(\eta_e)$
1	27	18.57	--
2	69	11,96	0.47
3	141	7.48	0.66
S_1 and S_2 enriched only			
p	DOF	η_e	$R(\eta_e)$
1	26	18.60	--
2	70	11.29	0.5
3	158	4.74	1.07
S_1 enriched only			
p	DOF	η_e	$R(\eta_e)$
1	25	51.49	--
2	71	36.79	0.32
3	163	29.44	0.27
S_0 enriched only			
Mesh	DOF	η_e	$R(\eta_e)$
1	25	64.05	--
2	71	56.00	0.13
3	163	52.83	0.07